Chemical Science

ROYAL SOCIETY OF CHEMISTRY | Celebrating IYPT 2019

EDGE ARTICLE
Junjie Fu, Jian Yin *et al.*
Introduction of the α-ketoamide structure: en route to develop hydrogen peroxide responsive prodrugs

Chemical Science

EDGE ARTICLE

Check for updates

Introduction of the α-ketoamide structure: en route to develop hydrogen peroxide responsive prodrugs†

Tingting Meng,‡[ab] Jing Han, [ID] ‡[c] Pengfei Zhang,[a] Jing Hu,[a] Junjie Fu [ID] *[ab] and Jian Yin*[a]

Leveraging the elevated levels of hydrogen peroxide (H_2O_2) in cancer, inflammatory diseases and cardiovascular disorders, H_2O_2-activated promoieties have been widely used in drugs and biomaterials design. However, the overwhelming majority of the promoieties only share the common structure of a H_2O_2-responsive arylboronic acid/ester moiety with low diversity. We report here an unprecedented strategy to construct novel H_2O_2-responsive prodrugs based on an α-ketoamide structure. As a proof of concept, we designed and synthesized a panel of α-ketoamide based nitrogen mustard prodrugs, among which **KAM-2** showed potent growth inhibitory activity and high selectivity toward cancer cells. The H_2O_2-trigged decomposition of **KAM-2** was validated, and the DNA damaging and apoptosis promoting activity attributed to the released nitrogen mustard were demonstrated. Our work unveils α-ketoamide as a new scaffold for prodrug design and may quickly inspire future developments.

Introduction

Prodrugs and probes, two important and vibrant research subjects in medicinal chemistry and analytical chemistry, are indeed closely related. Probes are usually trigged by specific analytes to release fluorescent signals, and prodrugs are activated by pathological stimuli to liberate drugs.[1,2] Importantly, chemists are always encouraged by the analyte-responsive moieties of probes and expand their applications to prodrug design to achieve spatiotemporal control of drug release. Recent examples include the intriguing discoveries of prodrugs activated by β-secretase,[3] histone deacetylase (HDAC)/cathepsin L (CTSL),[4] matrix metalloproteinase-7 (MMP-7),[5] caspase-3,[6] γ-glutamyl transferase,[7] thioredoxin reductase,[8] lysyloxidase,[9] photocleavage,[10] hypochlorous acid,[11] *etc.*

H_2O_2 has been taken as an important molecule due to its elevated levels in many pathological conditions.[12,13] The pioneer work from Chang *et al.*,[14,15] who initiated fluorescent probes bearing a H_2O_2-responsive boronate trigger in 2004–2005, led to the rapid expansion of this strategy to the design of H_2O_2-

activated prochelators and MMP proinhibitors.[16,17] Given the significantly high H_2O_2 concentrations (5–1000 μM) in cancer cells relative to normal cells (0.001–0.7 μM), Peng *et al.*,[18] for the first time, reported boron-based nitrogen mustard precursors as selective anticancer agents in 2011, followed by the blooming of various prodrugs (over 50 published papers) bearing an arylboronic acid/ester as the H_2O_2-cleavable trigger between 2012–2019 (Table S1†). Other H_2O_2-responsive moieties, such as arylsulfonyl ester,[19] thiazolidinone,[20] and benzothiazole[21] have also been reported for constructing small molecule prodrugs, but with very limited examples of each. In addition, sulfide, thioether, thioketal, selenium, and peroxalate ester are also known as H_2O_2-sensitive scaffolds, but in most cases, their applications are confined to polymers or nanoparticles.[22,23] As yet, currently over 90% H_2O_2-activated small molecule prodrugs still rely on the long-known boron-based triggers. Moreover, several disadvantages have been reported for the boron moiety, such as the high susceptibility of boronic esters to hydrolysis,[24] the off-target reactions between boronic acids and biological diols,[25] the moderate selectivity toward H_2O_2 and interference from $ONOO^-$, as well as the potential unknown bioeffects from the by-produced boric acid.[21] Considering the extremely low structural diversity of the current H_2O_2-responsive prodrugs, we have been highly interested in searching for novel chemical structures with H_2O_2-cleavable property.

We were recently enlightened by the elegant work from Tang *et al.*, who used α-ketoamide-based fluorescent probes for intracellular H_2O_2 visualization.[26–28] The α-ketoamide moiety was demonstrated as a highly specific reaction switch for H_2O_2. Herein, as a proof-of-concept, we introduce the α-ketoamide

[a]*Key Laboratory of Carbohydrate Chemistry and Biotechnology, Ministry of Education, School of Biotechnology, Jiangnan University, Wuxi 214122, P. R. China. E-mail: jfu@jiangnan.edu.cn; jianyin@jiangnan.edu.cn*

[b]*School of Pharmacy, Nanjing Medical University, Nanjing 211166, P. R. China*

[c]*School of Chemistry & Materials Science, Jiangsu Key Laboratory of Green Synthetic Chemistry for Functional Materials, Jiangsu Normal University, Xuzhou 221116, P. R. China*

† Electronic supplementary information (ESI) available. See DOI: 10.1039/c9sc00910h

‡ These authors contributed equally.

group into prodrug design by hybridizing it with nitrogen mustards, affording a panel of α-ketoamide-based nitrogen mustard (KAM) prodrugs. Multiple assays confirmed that one of the prodrugs, **KAM-2**, was efficiently and preferentially activated by H_2O_2, and showed potent and selective cytotoxicity to several cancer cell lines, particularly for HL-60 human leukemia cells. The ability of **KAM-2** to induce DNA damage and apoptosis was thoroughly studied. To the best of our knowledge, this is the first example to utilize the α-ketoamide moiety as an alternative non-boron H_2O_2-responsive element for prodrug development.

Results and discussion

Design and synthesis of KAM prodrugs

The structures of KAM prodrugs are illustrated in Scheme 1. It is speculated that the α-ketoamide moiety in **KAM-1**–**KAM-4** acts as an electron-withdrawing group and shields the activity of nitrogen mustards.[18,29–31] Upon the nucleophilic attack by H_2O_2 anion and the following Baeyer–Villiger rearrangement,[27] the promoiety finally hydrolyses into aniline nitrogen mustards with increased nitrogen electron density and restored DNA alkylating activity. To enrich the structural diversity, quaternary ammonia salts **KAM-5** and **KAM-6** were also designed as masked mustard prodrugs. The activation process of **KAM-5** and **KAM-6** are similar to the mechanism described above but require an additional spontaneous 1,6-elimination.[32]

The synthetic route (Scheme 2) of the target compounds commenced with a SeO_2-mediated oxidation of acetophenone in pyridine to afford phenylglyoxylic acid **1**, which was coupled with *N*-4-aminophenyl-diethanolamine or (4-aminophenyl) methanol in the presence of EDCI and DIEA to give α-ketoamides **2** or **3**, respectively. The two hydroxy groups of **2** were methylated to generate **KAM-3**. Further dichlorination, dibromination, and monochlorination of **KAM-3** furnished **KAM-1**, **KAM-2**, and **KAM-4**, respectively. Bromination of the hydroxy
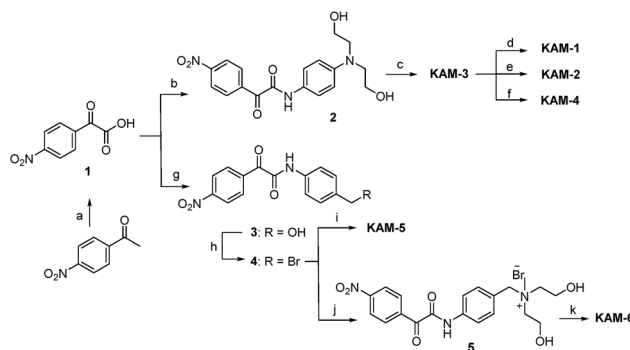

Scheme 2 Synthesis of KAM prodrugs. Reactants and conditions: (a) SeO_2, pyridine, 90 °C, N_2, 35%; (b) *N*-4-aminophenyl diethanolamine, EDCI, DIEA, DMF, 42%; (c) MsCl, DMAP, TEA, DCM, reflux, 70%; (d) LiCl (5 eq.), DMF, 60 °C, 65%; (e) NaBr (5 eq.), DMF, 60 °C, 67%; (f) LiCl (1 eq.), MeCN, 60 °C, 23%; (g) (4-aminophenyl)methanol, EDCI, DIEA, DMF, 33%; (h) CBr_4, PPh_3, DCM, 0 °C–r.t., 50%; (i) *N*-(4-*N'*,*N'*-dimethylaminophenyl)-bis(2-chloroethyl)amine, MeCN, 43%; (j) *N*-methyldiethanolamine, $CHCl_3$, reflux, 76%; (k) $SOCl_2$, r.t., 62%.

group of **3** using CBr_4 and PPh_3 yielded **4**, which was then directly reacted with aniline nitrogen mustard to give **KAM-5**. Alternatively, nucleophilic substitution of **4** with *N*-methyldiethanolamine, followed by chlorination with $SOCl_2$ generated **KAM-6**. Detailed synthetic procedures and spectroscopic data are provided in the ESI.†

Anticancer activity screening

The antiproliferative activity of KAM prodrugs was screened against four human cancer cell lines (A549, HepG2, HCT-116, and HL-60), which have all been well-employed in H_2O_2 responsive prodrug studies.[33–35] The classical nitrogen mustard mechlorethamine (MEC) was selected as the positive control. Evidently, **KAM-2** exhibited the most potent activity among all the candidates (Fig. 1). At a dose of 10 μM, the inhibition rates of **KAM-2** in all cancer cells were >50%, which further exceeded 80% at 20 μM. Structurally similar prodrugs **KAM-3** and **KAM-4** showed decreased cytotoxicity compared with **KAM-2**. The activity of chlorine counterpart, **KAM-1**, was further compromised. These results suggest that the leaving groups of mustard significantly affect the anticancer activity of KAM prodrugs. Ammonia salts **KAM-5** and **KAM-6** showed limited inhibition effects, particularly for **KAM-5**, possibly due to their lower membrane permeability and absorption.[30] This assumption was preliminarily tested by calculating the log P and membrane permeability values of KAM prodrugs, and the results are summarized in Table S2.† Considering the essential role of the nitro group of KAM in H_2O_2-initiated nucleophilic attack,[26,27] a non-nitro analogue **KAM-7** was synthesized (ESI†) as a negative control, which was supposed to be resistant to H_2O_2. As expected, **KAM-7** displayed diminished cytotoxicity against cancer cells (Fig. 1), demonstrating the role of H_2O_2 in prodrug activation.

The anticancer activity of **KAM-2** was then more closely studied by measuring its IC_{50} values, employing three additional H_2O_2-overproducing cancer cell lines (SW620, MCF-7,
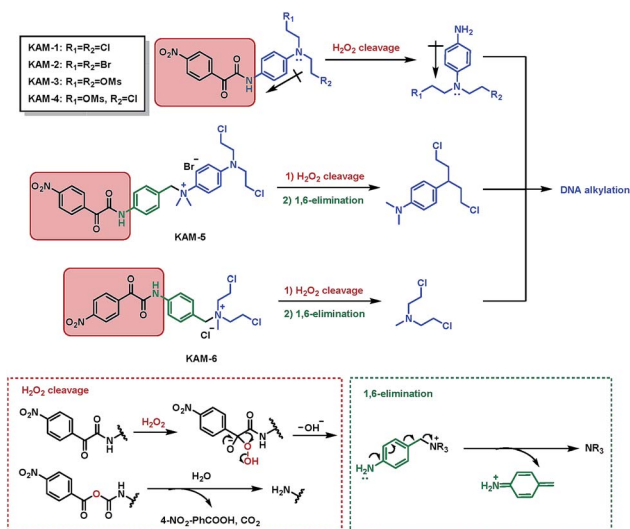
Scheme 1 Structures of KAM prodrugs and the mechanisms of H_2O_2-responsive activation to generate DNA alkylating agents.
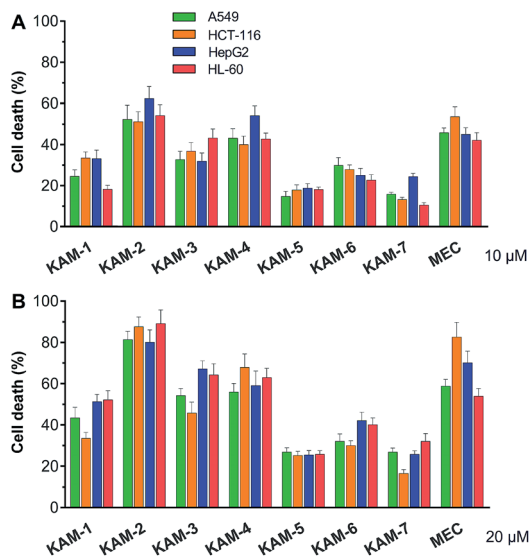
Fig. 1 Cytotoxicity of KAM prodrugs against four human cancer cell lines. Cells were incubated with indicated compounds at 10 (A) and 20 µM (B) for 72 h, and the percentages of cell death were assessed by MTT and CCK-8 assays. Mean ± SD, $n = 3$.

PANC-1)[36–38] plus one normal line, peripheral blood mononuclear cell (PBMC) (Fig. S1†). As summarized in Table 1, **KAM-2** showed lower IC_{50} values than MEC in cancer cells, except for PANC-1, which was particularly sensitive to MEC. The lowest IC_{50} (5.942 µM) of **KAM-2** was seen in HL-60 cell. Encouragingly, **KAM-2** proved its excellent selectivity toward cancer cells since the IC_{50} value in PBMC was larger than 50 µM. In contrast, MEC remained cytotoxic in PBMC with an IC_{50} value of 11.50 µM.

H_2O_2-responsive behaviours

All the KAM prodrugs decomposed quickly upon H_2O_2 treatment (Fig. S2A†). Considering the good cytotoxicity and selectivity of **KAM-2** toward cancer cells, its H_2O_2-responsive behaviours were in-depth studied. **KAM-2** exhibited a decent stability in the absence of H_2O_2 at pH 4, 7, 10, respectively

Table 1 IC_{50} values (µM) of **KAM-2** and MEC against selected cell lines[a]

Cell lines	IC_{50} (µM)	
	KAM-2	MEC
A549	8.82 ± 0.83	10.07 ± 0.71
HCT-116	8.01 ± 0.85	13.25 ± 1.57
HepG2	8.84 ± 1.24	10.68 ± 1.52
HL-60	5.94 ± 0.94	12.60 ± 3.47
MCF-7	12.19 ± 1.55	24.26 ± 1.23
PANC-1	16.25 ± 1.15	2.19 ± 0.08
SW620	9.10 ± 0.27	18.50 ± 0.07
PBMC	>50	11.50 ± 0.94

[a] Cells were incubated with indicated compounds at different concentrations for 72 h, and IC_{50} values were measured by MTT and CCK-8 assays. Mean ± SD, $n = 3$.

(Fig. S2B and S2C†). H_2O_2 rapidly triggered the decomposition of **KAM-2** in a H_2O_2 equivalent-dependent way (Fig. S2D†). As monitored by HPLC, the released nitrogen mustard N,N-bis(2-bromoethyl)benzene-1,4-diamine (BrM), as well as the by-product p-nitrobenzoic acid (PNB), were clearly observed 60 min after H_2O_2 treatment (Fig. 2A). In sharp contrast, **KAM-7** remained intact regardless of H_2O_2 presence (Fig. 2B and S2E†). The decomposition of **KAM-2** in H_2O_2 was further studied by ^1H NMR and mass spectroscopy, both of which unambiguously confirmed the prodrug activation behaviour (Fig. S3 and S4†). It is worth noting that in both HPLC and NMR studies, the signal of BrM shrank with time and became barely visible after long time treatment with H_2O_2. This is highly possible due to the instability of the phenylenediamine mustard toward H_2O_2 oxidation[39,40] under the in vitro study conditions, as shown in Fig. S5 and S6.† To provide a visual demonstration of the mustard release from **KAM-2**, BrM was prepared as a yellow solution, which turned dark upon H_2O_2 addition. The same colour change was observed with **KAM-2**/H_2O_2, but not with **KAM-7**/H_2O_2 (Fig. S7†). Moreover, in HL-60 cells, H_2O_2 scavenger N-acetyl-cysteine (NAC) pretreatment remarkably decreased the cytotoxicity of **KAM-2**, but not **KAM-7** (Fig. 2C). All the above results clearly demonstrated the H_2O_2-responsive activation of **KAM-2**. In regards of selectivity, **KAM-2** was resistant to HO$^•$, ^{t}BuO$^•$, TBHB, NO, GSH, and Fe^{2+}, very stable in ClO^-, Cys and Hcy. Slight decomposition was observed in $ONOO^-$, but to a much lesser extent than in H_2O_2 (Fig. 2D).

Proapoptotic mechanism of KAM-2

The anticancer activity of **KAM-2** was further evaluated in HL-60 cells using MEC as positive control. It was found that **KAM-2** treatment for 48 h induced apoptosis (Fig. 3A and S8A†) of HL-60 cells in a dose-dependent manner. Notably, NAC
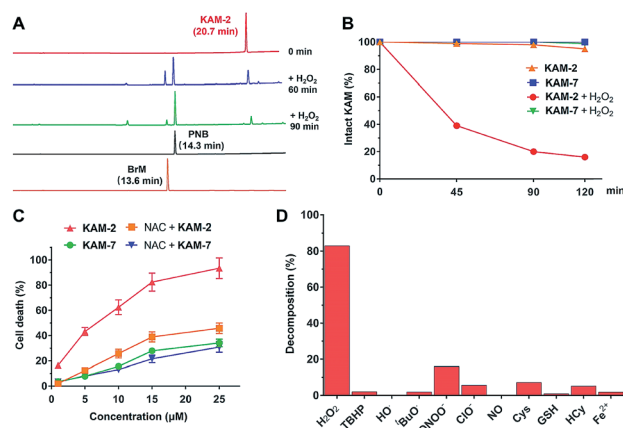

Fig. 2 H_2O_2-responsive behaviours of **KAM-2**. (A) Decomposition of 100 µM **KAM-2** in presence of H_2O_2 (2 eq.) as monitored by RP-HPLC (254 nm). (B) Decomposition of **KAM-2** and **KAM-7** (100 µM) with or without H_2O_2 (10 eq.). (C) The effects of NAC on the cytotoxicity of **KAM-2** and **KAM-7** in HL-60 cells after 72 h incubation. (D) Selectivity of **KAM-2** toward H_2O_2 as determined by measuring its decomposition ratios under various stimuli.
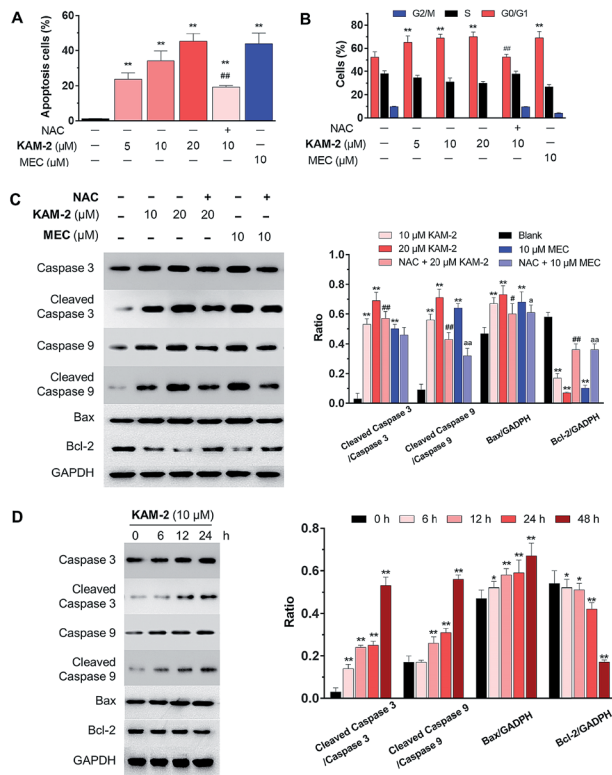
Fig. 3 (A) Apoptotic effects of **KAM-2** measured by flow cytometry using annexin V-FITC/PI staining. HL-60 cells were treated with compounds at indicated concentrations for 48 h, or pre-incubated with ROS scavenger NAC (20 mM) for 1 h, followed by treatment with 10 μM **KAM-2** for 48 h. Mean ± SD, $n = 3$. (B) Effects of **KAM-2** on cell cycle arrest. HL-60 cells were treated with compounds at indicated concentrations for 48 h, or pre-incubated with NAC (20 mM) for 1 h, followed by treatment with 10 μM **KAM-2** for 48 h. The percentage of cells in each cell cycle phase was analyzed by flow cytometry, mean ± SD, $n = 3$. (C) Dose-dependent effects of **KAM-2** on the expression of apoptosis-related proteins by Western blot. HL-60 cells were treated with compounds at indicated concentrations for 48 h or pre-incubated with NAC (20 mM) for 1 h, followed by treatment with compounds for 48 h. Mean ± SD, $n = 3$. $^{**}p < 0.01$ vs. blank; $^{\#}p < 0.05$ vs. 20 μM **KAM-2** treatment; $^{\#\#}p < 0.01$ vs. 20 μM **KAM-2** treatment; $^{a}p < 0.05$ vs. 10 μM MEC treatment; $^{aa}p < 0.01$ vs. 10 μM MEC treatment. (D) Time-dependent effects of **KAM-2** on the expression of apoptosis-related proteins by Western blot. HL-60 cells were treated with 10 μM **KAM-2** for 0, 6, 12, 24, and 48 h. Mean ± SD, $n = 3$. $^{*}p < 0.05$ vs. 0 h; $^{**}p < 0.01$ vs. 0 h.

pretreatment significantly decreased the activity of **KAM-2**. Neither **KAM-7** nor NAC showed apoptosis-inducing activity under the same condition (Fig. S8B†). Moreover, **KAM-2** arrested cell cycle in G0/G1 phase and NAC reversed the cell cycle arrest (Fig. 3B and S9†). Modest effects of **KAM-2** on the loss of mitochondrial membrane potential were also observed (Fig. S10†). Western blot studies revealed that **KAM-2** induced the cleavage of caspase 3 and caspase 9, elevated the expression of Bax, and suppressed the expression of Bcl-2 in a dose (Fig. 3C) and time (Fig. 3D) dependent way, similar to the effects of MEC. The above results suggest that **KAM-2** acts at least partially through the mitochondria-mediated apoptosis pathway.

DNA cross-linking and damaging effects of KAM-2

In addition to the above disclosed mechanism, the nitrogen mustard released from **KAM-2** upon H_2O_2 activation is supposed to exert its cytotoxicity by DNA interstrand cross-linking (ICL).[41] This was first examined by a fluorescence quenching experiment. It is known that ethidium bromide (EB) interacts with DNA to yield maximum fluorescence emission at 600 nm ($E_x = 300$ nm), which is supposed to be quenched due to competitive binding of nitrogen mustard to DNA. As expected, **KAM-2** decreased the fluorescence intensity at 600 nm in the presence of H_2O_2 (Fig. 4).

The DCL ability of activated **KAM-2** was further confirmed by denaturing alkaline agarose gel electrophoresis.[42] As shown in Fig. 5A and B, **KAM-2** or H_2O_2 alone had no effects on linearized pBR322 plasmid DNA. However, in the presence of 10 mM H_2O_2, **KAM-2** treatment induced DNA ICL (from 3.3% to 94.8%) as indicated by the intensified bands of double strand DNA (dsDNA) in both a dose and time dependent way. In contrast, **KAM-7** combined with H_2O_2 was unable to yield dsDNA (Fig. 5C). These results again, strongly support the H_2O_2-triggered activation of **KAM-2** and consequent generation of nitrogen mustard.

Next, the DNA damaging activity of **KAM-2** was assessed in HL-60 cells using comet assay. **KAM-2** treatment resulted in obvious cellular DNA damage as visually shown in Fig. 6. NAC preincubation protected HL-60 cells from tail DNA formation due to diminished activation of **KAM-2**. **KAM-7** or NAC alone had no effects on DNA damage (Fig. S11†).

Following DNA double-strand break (DSB), histone H_2AX is rapidly phosphorylated at Ser_{139} to yield γ-H_2AX as a golden biomarker of DNA damage response (DDR).[43] The expression of γ-H_2AX upon **KAM-2** treatment was therefore examined using immunofluorescence microscopy. Incubation of HL-60 cells with **KAM-2** for 12 h remarkably increased the level of γ-H_2AX (Fig. 7). Notably, when **KAM-2** was removed and cells were allowed to grow without **KAM-2** for an additional 6 or 12 h, elevated expression of γ-H_2AX was still observed. However, NAC pretreatment mitigated the effects of **KAM-2** on γ-H_2AX
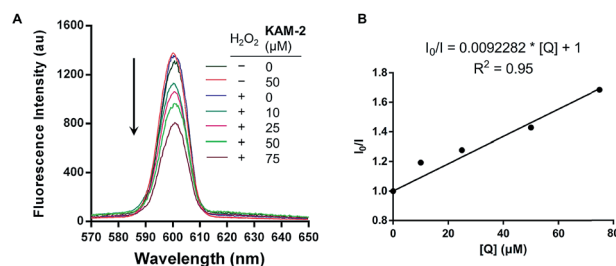

Fig. 4 (A) Fluorescence quenching of EB/DNA by **KAM-2**. Various concentrations of **KAM-2** was added into EB-DNA solution (2.5 μM EB and 50 μM linearized pBR322 plasmid DNA) with or without H_2O_2 (10 mM) in Tris−HCl/NaCl buffer. $E_x = 300$ nm (B) Stern−Volmer plots of fluorescence quenching of EB-DNA by **KAM-2**. I_0 and I are the emission intensity in the absence and presence of the **KAM-2**, respectively. Slope (K_{sv}) is the quenching rate constant, and [Q] is the concentration of the quencher **KAM-2**.
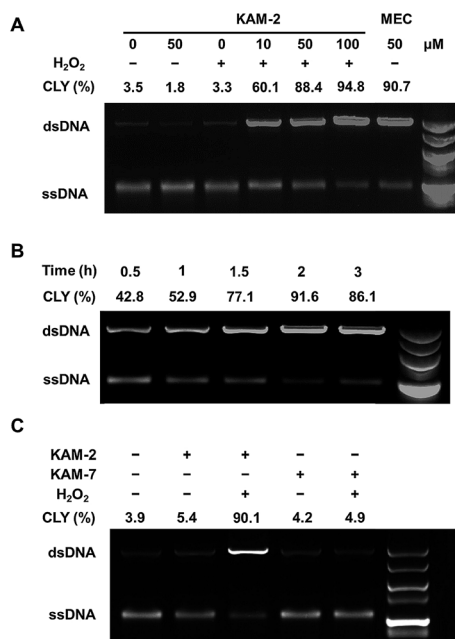
Fig. 5 DNA interstrand cross-linking (ICL) ability of **KAM-2**. (A) Denaturing alkaline agarose gel electrophoresis performed with 1 μg linearized pBR322 plasmid DNA and indicated concentrations of **KAM-2** or MEC with or without H_2O_2 (10 mM) for 2 h at 37 °C. (B) Denaturing alkaline agarose gel electrophoresis performed with 1 μg linearized pBR322 plasmid DNA, 50 μM **KAM-2**, and 10 mM H_2O_2 at 37 °C for indicated time. (C) Denaturing alkaline agarose gel electrophoresis performed with 1 μg pBR322, 50 μM **KAM-2** or **KAM-7** with or without H_2O_2 (10 mM) for 2 h at 37 °C. CLY: cross-linking yield.

Fig. 7 Immunofluorescence of DNA cleavage protein γH$_2$AX. HL-60 cells were treated with **KAM-2** or MEC (10 μM) for 12 h, or pre-incubated with ROS scavenger NAC (20 mM) for 1 h, followed by treatment with **KAM-2** for 12 h. For some groups, cells were incubated for an additional 6 or 12 h after removal of **KAM-2**.

formation. Compared with **KAM-2**, **KAM-7** and NAC had negligible effects on γ-H$_2$AX formation as shown in Fig. S12.†

In addition to γ-H$_2$AX, poly(ADP-ribose) polymerase-1 (PARP1), RAD51 and BRCA1 are activated by DNA DSB and involved in DNA repair.[44] The changes of PARP1, RAD51, BRCA1, and γ-H$_2$AX were quantified by Western blot. Clearly, **KAM-2** induced the cleavage of PARP1 and increased the expression of γ-H$_2$AX, RAD51 and BRCA1 in a dose (Fig. 8A) and

time (Fig. 8B) dependent way. In contrast, **KAM-7** or NAC treatment led to no alterations of the expressions of cleaved PARP1 or γ-H$_2$AX (Fig. S13†).

Fig. 8 (A) Concentration-dependent effects of **KAM-2** on the expression of DDR-related proteins by Western blot. HL-60 cells were treated with compounds at indicated concentrations for 48 h or pre-incubated with NAC (20 mM) for 1 h, followed by treatment with compounds for 48 h. Mean ± SD, $n = 3$. $^{**}p < 0.01$ vs. blank; $^{#}p < 0.05$ vs. 20 μM **KAM-2** treatment; $^{##}p < 0.01$ vs. 20 μM **KAM-2** treatment. (B) Time-dependent effects of **KAM-2** on the expression of DDR-related proteins by Western blot. HL-60 cells were treated with 10 μM **KAM-2** for 0, 6, 12, 24, and 48 h. Mean ± SD, $n = 3$. $^{*}p < 0.05$ vs. 0 h; $^{**}p < 0.01$ vs. 0 h.
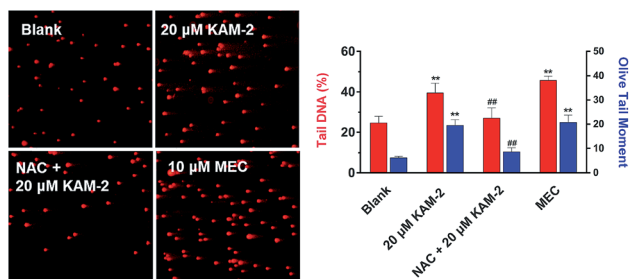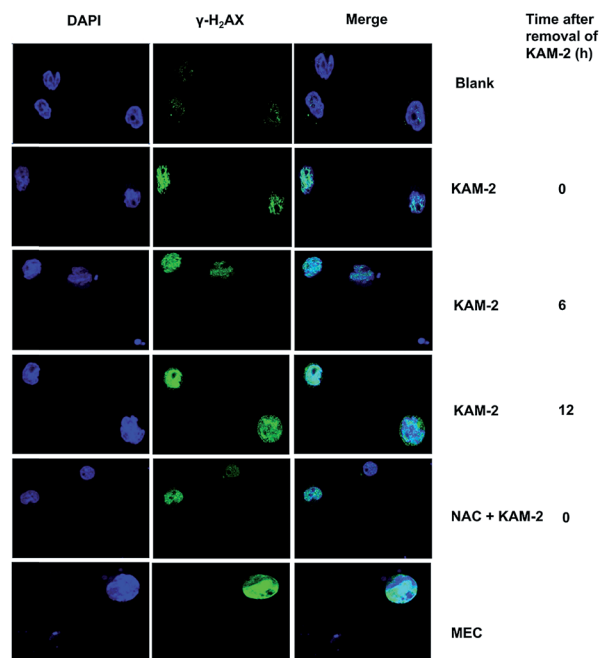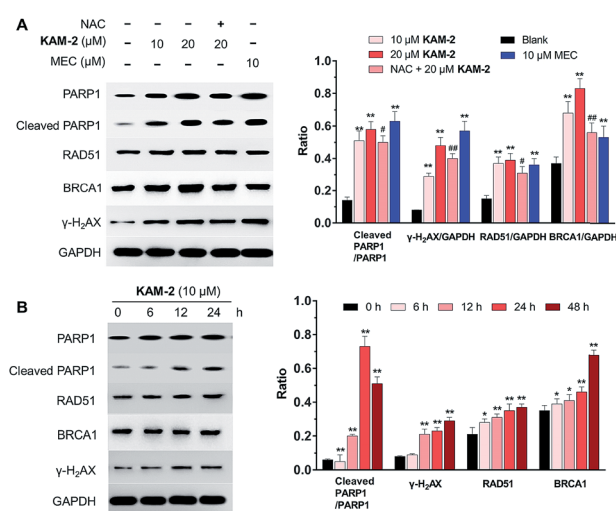

Fig. 6 Effects of **KAM-2** on cell damage assessed by comet assay. HL-60 cells were treated with 20 μM **KAM-2** or 10 μM MEC for 48 h, or pre-incubated with NAC (20 mM) for 1 h, followed by treatment with 10 μM **KAM-2** for 48 h. Alkaline comet electrophoresis was performed. Quantitative analysis was conducted with the comet analysis software CASP. The tail DNA% and olive tail moment were employed to evaluate DNA damage. Mean ± SD, $n = 3$. $^{**}p < 0.01$ vs. blank; $^{##}p < 0.01$ vs. 20 μM **KAM-2** treatment.
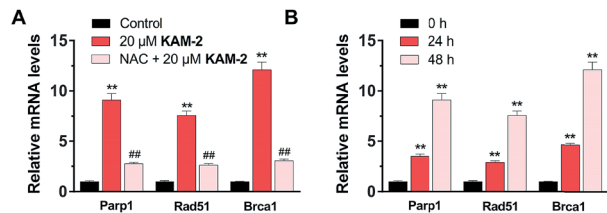
Fig. 9 The concentration- (A) and time-dependent (B) effects of 20 μM KAM-2 on the expression DDR-related mRNA levels tested by real-time PCR. Mean ± SD, $n = 3$. $^{**}p < 0.01$ vs. control or 0 h treatment; $^{##}p < 0.01$ vs. 20 μM KAM-2 treatment.

Finally, the effects of **KAM-2** on the expression of Parp1, Rad51 and Brca1 mRNAs were investigated in HL-60 cells. Real-time PCR assay confirmed that **KAM-2** concentration (Fig. 9A) and time (Fig. 9B) dependently elevated the mRNA expression levels of Parp-1, Rad51 and Brca1. Importantly, NAC pretreatment mitigated the effects of **KAM-2** on gene expression.

Conclusions

In summary, we for the first time present an α-ketoamide scaffold to build up H_2O_2-activated prodrugs, using nitrogen mustard as the model drug. Our studies identified **KAM-2** as a novel anticancer prodrug deserving further investigations. **KAM-2** obviously inhibited the growth of different cancer cell lines with diminished cytotoxicity in normal PBMC cells. The H_2O_2-induced decomposition of **KAM-2** was confirmed using various analytical methods. The nitrogen mustard released from **KAM-2** exhibited DNA ICL ability, led to DNA damage in HL-60 cells, and increased the expression of DDR related proteins and mRNAs. Additional mechanism studies suggested that **KAM-2** induced HL-60 apoptosis in a mitochondrial-dependent manner. In addition to the emerged boron-based H_2O_2-responsive prodrugs, our work showcases the establishment of a new platform for prodrug design inspired from analytical probes. Considering the close involvement of H_2O_2 in many pathological diseases, it is anticipated that our results will actively promote the development of both small molecule and nanoparticle-based agents in related fields.

Conflicts of interest

There are no conflicts to declare.

Acknowledgements

Notes and references

1 J. Rautio, N. A. Meanwell, L. Di and M. J. Hageman, *Nat. Rev. Drug Discovery*, 2018, **17**, 559.

2 S. H. Alamudi and Y. T. Chang, *Chem. Commun.*, 2018, **54**, 13641.

3 D. S. Folk and K. J. Franz, *J. Am. Chem. Soc.*, 2010, **132**, 4994.

4 N. Ueki, S. Lee, N. S. Sampson and M. J. Hayman, *Nat. Commun.*, 2013, **4**, 2735.

5 A. Tanaka, Y. Fukuoka, Y. Morimoto, T. Honjo, D. Koda, M. Goto and T. Maruyama, *J. Am. Chem. Soc.*, 2015, **137**, 770.

6 S. W. Chung, J. U. Choi, Y. S. Cho, H. R. Kim, T. H. Won, P. Dimitrion, O. C. Jeon, S. W. Kim, I. S. Kim, S. Y. Kim and Y. Byun, *Adv. Sci.*, 2018, **5**, 1800368.

7 S. Bakthavatsalam, M. L. Sleeper, A. Dharani, D. J. George, T. Zhang and K. J. Franz, *Angew. Chem., Int. Ed.*, 2018, **57**, 12780.

8 X. Li, Y. Hou, X. Meng, C. Ge, H. Ma, J. Li and J. Fang, *Angew. Chem., Int. Ed.*, 2018, **57**, 6141.

9 F. Kang, J. Zhu, J. Wu, T. Lv, H. Xiang, J. Tian, Y. Zhang and Z. Huang, *Chem. Sci.*, 2018, **9**, 6893.

10 S. B. Salunke, J. A. Malla and P. Talukdar, *Angew. Chem., Int. Ed. Engl.*, 2019, **58**, 5354.

11 P. Wei, L. Liu, Y. Wen, G. Zhao, F. Xue, W. Yuan, R. Li, Y. Zhong, M. Zhang and T. Yi, *Angew. Chem., Int. Ed.*, 2019, **58**, 4547.

12 R. Radi, *Proc. Natl. Acad. Sci. U. S. A.*, 2018, **115**, 5839.

13 B. D'Autreaux and M. B. Toledano, *Nat. Rev. Mol. Cell Biol.*, 2007, **8**, 813.

14 M. C. Chang, A. Pralle, E. Y. Isacoff and C. J. Chang, *J. Am. Chem. Soc.*, 2004, **126**, 15392.

15 E. W. Miller, A. E. Albers, A. Pralle, E. Y. Isacoff and C. J. Chang, *J. Am. Chem. Soc.*, 2005, **127**, 16652.

16 L. K. Charkoudian, D. M. Pham and K. J. Franz, *J. Am. Chem. Soc.*, 2006, **128**, 12424.

17 J. L. M. Jourden and S. M. Cohen, *Angew. Chem., Int. Ed.*, 2010, **49**, 6795.

18 Y. Kuang, K. Baakrishnan, V. Gandhi and X. Peng, *J. Am. Chem. Soc.*, 2011, **133**, 19278.

19 K. B. Daniel, J. L. M. Jourden, K. E. Negoescu and S. M. Cohen, *J. Biol. Inorg Chem.*, 2011, **16**, 313.

20 C. Perez, J.-P. Monserrat, Y. Chen and S. M. Cohen, *Chem. Commun.*, 2015, **51**, 7116.

21 C. K. Wang, J. Cheng, X. G. Liang, C. Tan, Q. Jiang, Y. Z. Hu, Y. M. Lu, K. Fukunaga, F. Han and X. Li, *Theranostics*, 2017, **7**, 3803.

22 C. Tapeinos and A. Pandit, *Adv. Mater.*, 2016, **28**, 5553.

23 G. Saravanakumar, J. Kim and W. J. Kim, *Adv. Sci.*, 2017, **4**, 1600124.

24 C. Achilli, A. Ciana, M. Fagnoni, C. Balduini and G. Minetti, *Cent. Eur. J. Chem.*, 2013, **11**, 137.

25 Y. Furikado, T. Nagahata, T. Okamoto, T. Sugaya, S. Iwatsuki, M. Inamo, H. D. Takagi, A. Odani and K. Ishihara, *Chem.–Eur. J.*, 2014, **20**, 13194.

26 C. Gao, Y. Tian, R. Zhang, J. Jing and X. Zhang, *Anal. Chem.*, 2017, **89**, 12945.

27 X. Xie, X. Yang, T. Wu, Y. Li, M. Li, Q. Tan, X. Wang and B. Tang, *Anal. Chem.*, 2016, **88**, 8019.

28 P. Gao, W. Pan, N. Li and B. Tang, *Chem. Sci.*, 2019, **10**, 6035.

29 S. Cao, Y. Wang and X. Peng, *Chem.–Eur. J.*, 2012, **18**, 3850.

30 W. Chen, K. Balakrishnan, Y. Kuang, Y. Han, M. Fu, V. Gandhi and X. Peng, *J. Med. Chem.*, 2014, **57**, 4498.

31 W. Chen, H. Fan, K. Balakrishnan, Y. Wang, H. Sun, Y. Fan, V. Gandhi, L. A. Arnold and X. Peng, *J. Med. Chem.*, 2018, **61**, 9132.

32 A. Alouane, R. Labruere, T. Le Saux, F. Schmidt and L. Jullien, *Angew. Chem., Int. Ed.*, 2015, **54**, 7492.

33 R. Kumar, J. Han, H. J. Lim, W. X. Ren, J. Y. Lim, J. H. Kim and J. S. Kim, *J. Am. Chem. Soc.*, 2014, **136**, 17836.

34 H. W. Liu, X. X. Hu, K. Li, Y. Liu, Q. Rong, L. Zhu, L. Yuan, F. L. Qu, X. B. Zhang and W. Tan, *Chem. Sci.*, 2017, **8**, 7689.

35 H. Hagen, P. Marzenell, E. Jentzsch, F. Wenz, M. R. Veldwijk and A. Mokhir, *J. Med. Chem.*, 2012, **55**, 924.

36 J. Noh, B. Kwon, E. Han, M. Park, W. Yang, W. Cho, W. Yoo, G. Khang and D. Lee, *Nat. Commun.*, 2015, **6**, 6907.

37 C. Q. Luo, Y. X. Zhou, T. J. Zhou, L. Xing, P. F. Cui, M. Sun, L. Jin, N. Lu and H. L. Jiang, *J. Controlled Release*, 2018, **274**, 56.

38 T. P. Szatrowski and C. F. Nathan, *Cancer Res.*, 1991, **51**, 794.

39 Z. Can, A. Uzer, K. Turkekul, E. Ercag and R. Apak, *Anal. Chem.*, 2015, **87**, 9589.

40 T. B. Zanoni, F. Hudari, A. Munnia, M. Peluso, R. W. Godschalk, M. V. Zanoni, G. J. den Hartog, A. Bast, S. B. Barros, S. S. Maria-Engler, G. J. Hageman and D. P. de Oliveira, *Toxicol. Lett.*, 2015, **239**, 194.

41 R. K. Singh, S. Kumar, D. N. Prasad and T. R. Bhardwaj, *Eur. J. Med. Chem.*, 2018, **151**, 401.

42 J. J. Tepe and R. M. Williams, *J. Am. Chem. Soc.*, 1999, **121**, 2951.

43 E. P. Rogakou, D. R. Pilch, A. H. Orr, V. S. Ivanova and W. M. Bonner, *J. Biol. Chem.*, 1998, **273**, 5858.

44 S. Ganesan and A. F. Keating, *Toxicol. Appl. Pharmacol.*, 2015, **282**, 252.